Accelerated Ovarian Aging in the Absence of the Transcription Regulator TAF4B in Mice 1

Authors: Lovasco, Lindsay A., Seymour, Kimberly A., Zafra, Kathleen, O'Brien, Colin W., Schorl, Christoph, et al.

Source: Biology of Reproduction, 82(1) : 23-34

Published By: Society for the Study of Reproduction

URL: https://doi.org/10.1095/biolreprod.109.077495

BIOLOGY OF REPRODUCTION **82,** 23–34 (2010)
Published online before print 14 August 2009.
DOI 10.1095/biolreprod.109.077495

Accelerated Ovarian Aging in the Absence of the Transcription Regulator TAF4B in Mice[1]

Lindsay A. Lovasco, Kimberly A. Seymour, Kathleen Zafra, Colin W. O'Brien, Christoph Schorl, and Richard N. Freiman[2]

Department of Molecular and Cell Biology and Biochemistry, Brown University, Providence, Rhode Island

ABSTRACT

The mammalian ovary is unique in that its reproductive life span is limited by oocyte quantity and quality. Oocytes are recruited from a finite pool of primordial follicles that are usually exhausted from the ovary during midadult life. If regulation of this pool is perturbed, the reproductive capacity of the ovary is compromised. TAF4B is a gonad-enriched subunit of the TFIID complex required for female fertility in mice. Previous characterization of TAF4B-deficient ovaries revealed several reproductive deficits that collectively result in infertility. However, the etiology of such fertility defects remains unknown. By assaying estrous cycle, ovarian pathology, and gene expression changes in young *Taf4b*-null female mice, we show that TAF4B-deficient female mice exhibit premature reproductive senescence. The rapid decline of ovarian function in *Taf4b*-null mice begins in early postnatal life, and follicle depletion is completed by 16 wk of age. To uncover differences in gene expression that may underlie accelerated ovarian aging, we compared genome-wide expression profiles of 3-wk-old, prepubescent *Taf4b*-null and wild-type ovaries. At 3 wk of age, decreased gene expression in *Taf4b*-null ovaries is similar to that seen in aged ovaries, revealing several molecular signatures of premature reproductive senescence, including reduced *Smc1b*. One significantly reduced transcript in the young TAF4B-null ovary codes for MOV10L1, a putative germline-specific RNA helicase that is related to the *Drosophila* RNA interference protein, armitage. We show here that *Mov10l1* is expressed in mouse oocytes and that its expression is sensitive to TAF4B level, linking TAF4B to the posttranscriptional control of ovarian gene expression.

aging, gene regulation, oocyte development, oogenesis, ovary, ovulatory cycle, TFIID, transcription

INTRODUCTION

The regulation of aging of the mammalian ovary is a complex process and unique among diverse organ systems. A key factor in determining the length of female mammalian reproductive life span is the number of primordial follicles present in the ovary at birth and the maintenance of this finite pool during early postnatal life. In women, ovarian life span is not always directed by chronological age [1]. Often, young women seeking treatment at fertility clinics display characteristics of advanced ovarian age, such as reduced primordial follicle pool and elevated follicle-stimulating hormone (FSH) level. When the follicle reserve is low in women, oocyte quality is low regardless of chronological age, resulting in an increased number of chromosomal abnormalities and miscarriages [2]. Diminished oocyte quality in older women seems to be the major hurdle in conception. A previous study demonstrated that older women could carry and bear children just as well as younger women if oocyte quality were controlled using oocytes donated by younger women [3]. Results of studies in mice are in agreement with observations in humans of diminished oocyte quality with advanced age and reveal that age-related increases in aneuploidy may be attributed to reduced transcript number of spindle assembly checkpoint genes [4]. Taken together, these data suggest that declining fertility with age reflects the declining quality of the oocyte and a depleted follicle pool.

Recent gene expression studies in mice have elucidated age-related gene expression changes in whole ovaries as well as oocyte-specific differences [5, 6]. Consistent with aging in other organs, aged ovaries showed increased levels of genes involved in immune functions and decreased levels of those associated with mitochondrial electron transport, but the majority of transcript changes were related to ovary-specific processes. These results highlight the unique modes of aging found within the ovary. A second important result from molecular profiling of aged oocytes was the alterations in expression patterns of genes encoding proteins involved in chromatin structure, genome stability, and RNA helicases. Thus, the regulation of gene expression might become increasingly impaired as oocytes age [5].

Many of the signaling factors controlling ovary function and reproductive aging are well known, but less is known about the mechanisms of transcriptional integrators and effectors of specific oogenic transcriptional networks. Recent characterization of the general transcription machinery has revealed gonad-specific or -enriched variants of general transcription factors required for gametogenesis in diverse organisms [7–9]. TFIID is a large multiprotein complex that includes the TATA-box binding protein (TBP) and numerous TBP-associated factors (TAFs), which function collectively as core promoter recognition factors and coactivators [10–12]. One variant general transcription factor that is essential for multiple aspects of mammalian gametogenesis is the gonad-enriched TAF4B subunit of TFIID. In the mouse, TAF4B is required for proper female and male fertility. Although dispensable for the first round of spermatogenesis in the mouse testis, TAF4B is required for subsequent rounds and maintenance of spermatogenesis in the early adult [13]. In contrast, female mice that do

[1]Supported by NIH/NCRR COBRE Award P20RR015578 and the Ellison Medical Foundation Junior Scholar Award in Aging to R.N.F. and the National Center of Excellence in Women's Health at Brown University.
[2]Correspondence: Richard N. Freiman, Department of Molecular, Cell Biology, and Biochemistry, Brown University, 70 Ship St., Box G-E4, Providence, RI 02903. FAX: 401 863 9653;
e-mail: richard_freiman@brown.edu

Received: 13 March 2009.
First decision: 15 April 2009.
Accepted: 29 July 2009.

eISSN: 1529-7268 http://www.biolreprod.org
ISSN: 0006-3363

not express *Taf4b* are completely infertile because of multiple defects of oogenesis, such as a reduced primordial follicle pool, increased granulosa cell apoptosis, decreased granulosa cell proliferation, and increased FSH levels recorded as early as 23 days of age [14–16]. *Taf4b* heterozygotes do not show an intermediate phenotype but are comparable to wild type with respect to fertility. Pseudopregnant *Taf4b*-null mice are able to successfully maintain pregnancy of implanted wild-type embryos, pointing to impairment before implantation. There also have been documented developmental defects in the oocytes derived from *Taf4b* knockout mice, which exhibit decreased ability to complete meiosis I, extrude a polar body, and cleave properly following fertilization [14]. Ovulation in the *Taf4b*-null mouse has been assessed under multiple conditions of hormonal stimulation, age, and copulation. The data are not completely consistent. However, there appears to be a reduced level of ovulation in *Taf4b*-null mice, although the underlying cause is not clear [14]. Conflicting reports of *Taf4b*-target gene expression and localization of TAF4B in ovarian cell types exist, but it is becoming apparent that the age at which these are assayed is of great importance. Taken together, these studies suggest that rather than play a very specific role in female fertility, TAF4B executes several related functions that coordinate multiple aspects of female fertility, including those regulated by the somatic and oocytic compartments of the ovary.

Poor oocyte quality, reduced primordial follicle pool, and elevated FSH in young *Taf4b*-null mice lead us to hypothesize that these mice may be experiencing aspects of premature reproductive senescence. Many of the initial defects observed in the adult TAF4B-null ovary, such as decreased expression of several genes important in folliculogenesis, are not observed in the prepubescent ovary, and cursory examination of the ovary suggests that the *Taf4b*-null phenotype worsens with age. Initial characterization of *Taf4b*-null mice included a microarray that compared wild-type and *Taf4b*-null ovarian gene expression in adult mice, at which point TAF4B-null ovaries are largely depleted of follicles and granulosa cell proliferation is impaired [15]. To examine further the potential role of TAF4B in the transcriptional control of ovarian life span regulation, we compared the estrous cycle, ovarian development, and gene expression profiles between prepubertal and adult TAF4B-null ovaries. Here, we show that in the absence of TAF4B, female mice prematurely enter and exit the estrous cycle compared to their corresponding wild-type counterparts and develop hemorrhagic cysts. Candidate gene expression assays showed that disrupted expression of a negative regulator of activin, follistatin (*Fst*), occurred between 2 and 3 wk of age in the TAF4B-null ovary and pituitary. Components of the AKT/FOXO/PTEN ovarian survival pathway were examined between juvenile and adult mice to determine if their misexpression was involved in TAF4B-null ovarian cell death. Genome-wide whole-ovary expression profiling at 3 wk of age revealed the reduced expression of NACHT, leucine-rich repeat and PYD-containing (NLRP or NALP) gene family members, and oocyte-specific genes that have been shown to change their expression levels in aged ovaries [5] as well as *Obox* gene family members, which are exclusively expressed in germ cells [17]. *Smc1b* and *Mad2l1*, important meiotic genes that show decreased expression with human maternal aging, also are decreased, as is the putative germline-specific RNA helicase, *Mov10l1*. We do not observe a global down-regulation of oocyte-specific genes, but the gene expression changes we see indicate that young TAF4B-null oocytes may be prematurely aged. In addition, these data suggest that deregulated TAF4B-dependent events may underlie premature reproductive senescence and infertility in women.

MATERIALS AND METHODS

Animals

Wild-type and *Taf4b*-null or heterozygous mice were generated by mating heterozygous *Taf4b*$^{+/-}$ male and female mice as described previously [15]. Offspring were genotyped by PCR analysis of tail-snip genomic DNA amplifying the region targeted by homologous recombination. Daily vaginal smear cytology was performed to determine estrous cycle stage. Mice were classified as in diestrus, proestrus, or estrus based on the majority cell type present in the vaginal sample. Estrous cycle entry was deemed to be opening of the vagina and presence of primary leukocytes in the sample. Samples in prepubescent mice were not taken if the vagina had not opened. No mouse was cycled for more than 27 consecutive days. All animal protocols were reviewed and approved by Brown University Institutional Animal Care and Use Committee and were performed in accordance with the National Institutes of Health Guide for the Care and Use of Laboratory Animals.

Ovarian Histology

Ovaries were removed, cleaned of excess fat and bursal sac, and fixed in Bouin solution overnight. Standard paraffin embedding, sectioning, and hematoxylin-and-eosin staining were performed. Images were taken using the Scanscope CS (Aperio).

Ovarian Cell Isolation

Oocyte isolation. Oocytes were collected from 8-wk-old wild-type mice as described by Ebert et al. [18]. Ovaries were removed, cleaned of excess fat and bursal sac, washed in PBS, and agitated in an enzyme solution (0.1% collagenase type 3 [Worthington], 0.02% DNase type I [Worthington], and 0.1% trypsin [Invitrogen] in Hanks balanced salt solution [Invitrogen]), for 30 min at 37°C. Ovaries were dispersed using a 20-G needle, the solution was diluted with Dulbecco modified Eagle medium/Ham F-12 (DMEM-F12), and oocytes free of cumulus cells were collected. Oocytes were washed once with PBS and resuspended in Trizol reagent (Bio-Rad) for subsequent RNA isolation. Ovaries of three mice (~120 oocytes) were combined per sample.

Granulosa cell isolation. Ovaries from 8-wk-old wild-type mice were removed, cleaned of excess fat and bursal sac, and placed in DMEM-F12. Granulosa cells were liberated by pricking with a 26-G needle. Resulting granulosa cell suspensions were passed through a 40-μm nylon filter to remove large tissue clumps and oocytes. Purified granulosa cells were washed once in PBS and resuspended in Trizol reagent for RNA isolation or in extraction buffer (0.2 M KCl, 0.1 M Tris [pH 8], 0. 2 mM ethylenediaminetetra-acetic acid [EDTA], 0.1% NP-40, 10% glycerol, and 1 mM PMSF) for protein isolation. Granulosa cells of two mice were combined per sample.

Whole ovary. Ovaries from 8-wk-old wild-type mice were removed, cleaned of excess fat and bursal sac, and Dounce homogenized in Trizol reagent for subsequent RNA isolation or in extraction buffer for protein isolation. Ovaries of one mouse were used per sample.

Western Blot Analysis

Whole ovaries were Dounce homogenized and soluble protein extracted in low-salt protein extraction buffer (0.2 M KCl, 0.1 M Tris [pH 8], 0.2 mM EDTA, 0.1% NP-40, 10% glycerol, and 1 mM PMSF). Protein concentration was determined by Bradford assay, and equivalent amounts of protein were loaded per lane. The following antibodies were used: from Cell Signaling Technologies, FOXO1 2880, Phospho-FOXO1 (Thr24)/FOXO3a (Thr32) 9464, FOXO3 9467, Phospho-FOXO3 (Ser253) 9466, Phospho-FOXO3 (Ser318/321) 9465, FOXO4 9472, AKT 9272, Phospho-AKT (Ser473) 9271, Phospho-AKT (Thr308) 9275, PTEN 9552, and Phospho-PTEN (Ser380/Thr382/383) 9554; from BD Transduction Laboratories, TAF4A (TAF135) 612054; from Novus Biologicals, β-Tubulin RB-9249-P; and from Santa Cruz Biotechnology, CDKN1B (C-19), sc-528.

Quantitative RT-PCR

Total RNA was isolated from indicated tissues using Qiagen RNeasy micro kits, and concentration was determined using a Nanodrop (Thermo Scientific). Twenty microliters of cDNA were prepared from approximately 500 ng of total RNA using iScript cDNA Synthesis Kit (Bio-Rad), according to the manufacturer's directions, using a mix of oligo(dT) and random primers. Real-time PCR reactions were performed in triplicate using 2 μl of cDNA template, ABI Power SYBR green PCR master-mix, and gene-specific primers in the ABI 7500 Real Time PCR System. Dissociation curves were generated,

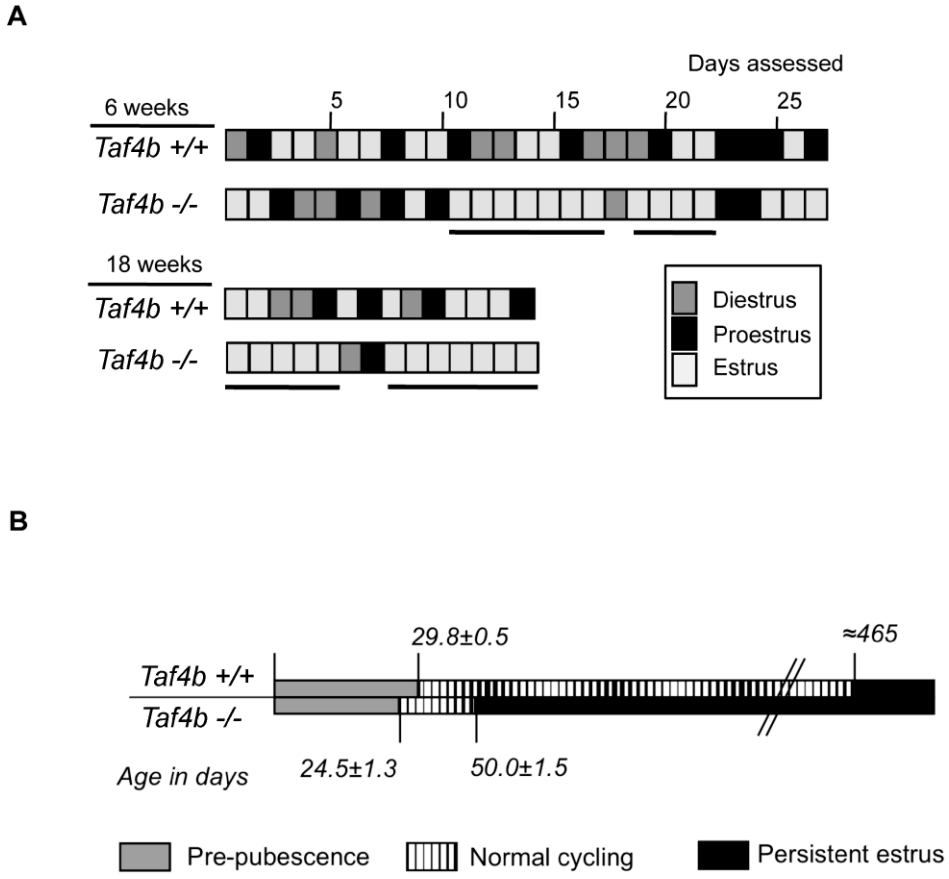

FIG. 1. Estrous cycle disruption in *Taf4b*-null mice. Vaginal smear cytology was performed daily to assess the estrous stage of *Taf4b*-null (−/−) and their wild-type (+/+) and heterozygous (+/−) littermates. **A**) Representative samples of wild-type and *Taf4b*-null mice, assessed daily, starting at 6 and 18 wk of age. Each block indicates the stage of the mouse for that day. Days indicating persistent estrus are underlined. **B**) Summary of wild-type ($Taf4b^{+/+}$) and *Taf4b*-null ($Taf4b^{-/-}$) estrous cycle with age at onset of puberty at 24.5 ± 1.3 days for *Taf4b*-null mice (n = 4) and 29.8 ± 0.5 days for wild-type mice (n = 4). *Taf4b*-null mice (n = 3) enter persistent estrus at 50 ± 1.5, whereas wild-type mice do not enter until approximately 465 days (15 mo) [20].

and PCR products were run on an agarose gel to verify amplification of a single product. Quantitative PCR data were analyzed by the ΔΔCt method. Relative expression levels were normalized to 18S ribosomal RNA levels to correct for equivalent total RNA levels. Primer sequences can be found in Supplemental Table S1 (all Supplemental Data are available online at www.biolreprod.org).

Microarray

Total RNA from nine 3-wk-old mice (n = 3 wild-type, 3 *Taf4b*-heterozygous, and 3 *Taf4b*-null mice) was obtained as described above. RNA quality was checked using a Bioanalyzer (Agilent), and concentration was determined using a Nanodrop. Three-hundred nanograms of each RNA sample were used in the Affymetrix Whole-Transcript Sense Target Labeling Assay (Rev 3), followed by hybridization to a GeneChip Mouse Gene 1.0 ST Array. Nine GeneChips were used to provide biological triplicates of each genotype. The Affymetrix Expression Console (v 1.1) was used to normalize data and determine signal intensity (RMA-Sketch). Analysis was performed in Microsoft Excel, and DAVID Bioinformatic software was used to identify gene expression pathways [19].

Small Interfering RNA-Mediated Gene Knockdown

The TAF4A and TAF4B SMARTpool siRNAs and ON-TARGET*plus* Non-Targeting Pool (mouse) were purchased from Dharmacon and transfected into the mouse GC1 cell line using Dharmafect reagent 1. Optimization was performed according to the manufacturer's instructions. Cells were harvested at 60 h posttransfection.

RESULTS

Estrous Cycle Disruption in Taf4b*-Null Mice*

High FSH levels are often associated with irregular cycling in mouse models of infertility and in both premature ovarian failure and menopause in women. *Taf4b*-null mice exhibit high levels of FSH as early as 3 wk of age; therefore, we set out to characterize the regularity of their estrous cycle. Daily examination of cell type by vaginal smear cytology revealed that *Taf4b*-null females have irregular cycling; a representative sample is shown in Figure 1A. Initial cycling trials, lasting from 11 to 27 days, were completed with sexually mature mice from 6 wk to 7 mo of age ($Taf4b^{-/-}$, n = 7; $Taf4b^{+/-}$, n = 9; $Taf4b^{+/+}$, n = 5). While all heterozygous and wild-type mice cycled appropriately, all *Taf4b*-null littermates were characterized as being in persistent estrus, exhibiting at least one period of more than 4 days stalled in estrus. Persistent estrus usually accompanies the natural reproductive senescence occurring around 15 mo (465 days) in wild-type C57BL/6 mice [20]. Surprisingly, 6-wk-old *Taf4b*-null mice displayed relatively normal cyclicity during the first week of sample collection, whereas older *Taf4b*-null mice spent the vast majority of time in estrus with sporadic and brief reentry into the estrous cycle.

Upon discovering that the younger *Taf4b*-null mice could temporarily cycle normally, we set out to better characterize estrous cycling at the onset of estrus. We examined litters beginning at 3 wk ($TAF4B^{-/-}$, n = 4; $TAF4B^{+/-}$, n = 4; $TAF4B^{+/+}$, n = 4), 4 wk ($TAF4B^{-/-}$, n = 1; $TAF4B^{+/-}$, n = 1), and 5 wk ($TAF4B^{-/-}$, n = 2; $TAF4B^{-/-}$, n = 1; $TAF4B^{+/+}$, n = 1) of age and found that females did not remain in estrus for periods of longer than 3 days until 6–7 wk of age, with persistent estrus occurring at Postnatal Day (pnd) 50 ± 1.5 (Fig. 1B). The timing of entry into estrus also is significantly earlier for *Taf4b*-null mice, with onset at pnd 24.5 ± 1.3, compared to onset at 28.2 ± 1.1 for *Taf4b*-heterozygotes and at pnd 29.8 ± 0.5 for wild types. Thus, defects in prepubertal *Taf4b*-null mice most likely lead to both accelerated activation and senescence of the TAF4B-deficient ovary. These data reveal a small window of normal cycling for *Taf4b*-null mice from an early onset at pnd 24.5 ± 1.3 to a state of persistent estrus beginning at pnd 50 ± 1.5 (Fig. 1B).

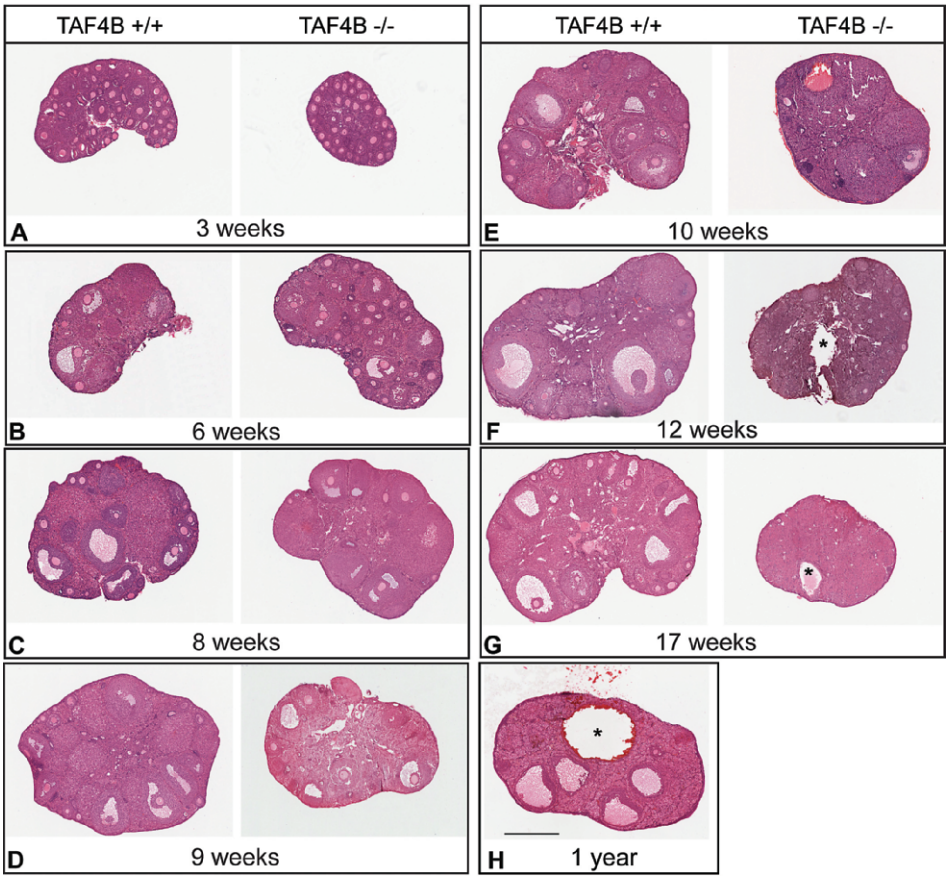

FIG. 2. Progressive follicle loss in TAF4B-null ovaries. **A**–**G**) Gross ovarian histology using hematoxylin-and-eosin staining of Bouin-fixed ovaries at 3 (**A**), 6 (**B**), 8 (**C**), 9 (**D**), 10 (**E**), 12 (**F**), and 17 (**G**) wk of age from *Taf4b*$^{-/-}$ mice and their wild-type (*Taf4b*$^{+/+}$) littermates shows the progressive and rapid loss of maturing oocytes. **H**) One-year-old wild-type ovary serves as a reference for normal aging in the C57BL/6 mouse line and shows the presence of both developing follicles and a hemorrhagic cyst. Asterisk indicates hemorrhagic cyst. Bar = 500 μm.

Histopathological Examination of TAF4B-Null Ovaries

Disruption of the estrous cycle in *Taf4b*-null mice suggested that follicular development may be similarly deregulated. Our previous study included a comprehensive count of follicle stages at 3, 6, and 12 wk of age and revealed that TAF4B-null ovaries contain reduced numbers of primordial follicles and increased atretic follicle number at each time point, whereas recruitment to the primary follicle stage is comparable to that in wild-type ovaries. We did not set out to uncover numerical follicle-stage data in the present study; instead, we turned to histopathological examination of the TAF4B-null ovary to capture its rapid degeneration. To better understand the effects on the ovary during the progression from normal to irregular cycling, we harvested TAF4B-null and matched wild-type ovaries between 3 and 17 wk of age for histological staining. From 3 wk of age (before puberty and hormonal signaling has commenced in wild-type mice) until sexual maturity at 8 wk, ovaries from *Taf4b*-null and wild-type mice were indistinguishable (Fig. 2, A–C). At 8 wk, TAF4B-null ovaries contained healthy antral follicles, which is interesting given that these mice were beginning to cycle irregularly (Fig. 2C). Strikingly, only 1 wk later, at 9 wk of age, the TAF4B-null ovaries displayed obvious signs of premature depletion of follicles (Fig. 2D). By 10 wk, the TAF4B-null ovary contained very few oocytes (Fig. 2E). By 12 wk, hemorrhagic cysts became evident (Fig. 2F), and many fragmented oocytes were present in degenerating follicles (Supplemental Fig. S1). The 17-wk-old TAF4B-null ovary appeared to be devoid of all developing follicles and oocytes (Fig. 2G). In contrast, the wild-type ovary still contained some healthy follicles at 1 yr of age and beyond (Fig. 2H). We also observed an increased occurrence of hemorrhagic cysts in the *Taf4b*-null mice. TAF4B-null ovaries were observed with one, two, or multiple cysts, with the earliest identified at 16 wk of age. The ovaries collected from an aged wild-type mouse contained multiple cysts resembling those of the younger *Taf4b*-null animals (Supplemental Fig. S2). Taken together, these data indicate that follicular development is relatively intact, whereas the *Taf4b*-null mice are cycling normally and premature depletion of all follicles occurs rapidly by 17 wk. Additionally, early cyst formation closely follows the onset of persistent estrus.

Progressive Loss of the AKT Survival Pathway in TAF4B-Deficient Ovaries

The rapid depletion of follicles led us to investigate the possible role of a disrupted AKT survival pathway in the TAF4B-deficient ovary. At 4 wk, all of the total and phosphorylated FOXO proteins tested were present at near-equivalent levels between the wild-type and TAF4B-null ovary (Fig. 3A). In 16-wk-old TAF4B-null ovaries, FOXO1 and phosphorylated FOXO3 were almost undetectable, whereas total FOXO3 and FOXO4 were present but with reduced levels. Although almost complete loss of FOXO3 phosphorylation was found in the 16-wk-old TAF4B-null ovary, only an approximately 50% loss of total FOXO3 protein was found, suggesting that at 16 wk, phosphorylation of FOXO3 is reduced in TAF4B-null ovaries. Of the factors tested that are upstream of FOXO proteins in this survival pathway, we found a slight decrease in total AKT at 16 wk in the TAF4B-null ovary, accompanied by a very slight decreases in phosphorylated AKT (Fig. 3B). PTEN and p-PTEN were equivalent between genotypes at both 4 and 16 wk. Interestingly, CDKN1B (also known as p27) levels were equivalent at 4 wk and elevated in the 16-wk-old knockout. At the earliest time

point examined, defects in the AKT survival pathway were not prevalent, and these later defects may be the consequence, rather than the cause, of premature senescence of the TAF4B-null ovary.

To examine the relative levels of TFIID components between 4 and 16 wk, we used antibodies against TAF4, TAF4B, and TBP. Loss of TAF4B did not change levels of the paralogous TAF4 subunit in the ovary, which remained constant between genotypes at both time points. However, TBP was slightly reduced at 16 wk in the TAF4B-null ovary (Fig. 3C). Interestingly, the level of TAF4B in the wild-type ovary was elevated at 4 wk compared to 16 wk. Whereas 4 wk of age is just at, or before, the onset of estrus in a wild-type mouse, these mice were cycling regularly at 16 wk, so if TAF4B protein level were dynamic through the estrous cycle, this lower level may have been a result of examining the mouse in a phase during which TAF4B normally is low. To this end, we collected ovaries at different points during the estrous cycle and found that *Taf4b* mRNA and TAF4B protein expression do not change between estrus, diestrus, and proestrus (Supplemental Fig. S3). The elevated levels of TAF4B at 4 wk in wild-type ovaries may suggest a greater need for TAF4B action at early stages of ovarian function, a lack of which leads to premature senescence.

Follistatin mRNA Down-Regulation in TAF4B-Null Ovary and Pituitary

Similar to FOXO and AKT expression, many TAF4B-target genes were reduced in older, but not in younger, TAF4B-null ovaries. Although young TAF4B-null ovaries appeared to be healthy, without a complete TFIID complex there may be underlying transcriptional deregulation from early time points, which ultimately may lead to premature reproductive senescence. Previous data implicating TAF4B in control of *Fst* expression, combined with high FSH levels, led us to examine *Fst* expression between *Taf4b*-null mice and wild-type littermates. To determine if TAF4B is necessary for proper *Fst* expression, we performed quantitative RT-PCR on ovary-derived RNA. At 7 mo of age, when the TAF4B-null ovary contains no growing follicles, *Fst* mRNA levels were decreased between three- and sixfold compared to wild-type and heterozygous littermates (Fig. 4A). In addition to granulosa cells of the ovary, the anterior pituitary also produces *Fst*, which acts there as a paracrine signaling factor [21]. At 3 wk of age, *Fst* mRNA levels were significantly reduced by threefold in the TAF4B-null ovary (Fig. 4B) and by twofold in the pituitary (Fig. 4C). However, *Fst* misregulation is probably not the sole cause of the TAF4B-null female phenotype, because at 2 wk of age, *Fst* levels in the TAF4B-null ovary (Fig. 4D) and pituitary (data not shown) were equivalent to those of its heterozygous littermates. Regulation of other key pituitary factors, *Fshb*, *Inhbb,* and *Foxl2,* seemed to be largely intact (Fig. 4C). Follistatin, a key component in the ovary-pituitary axis, appeared to be deregulated in the *Taf4b*-null mouse, both in the ovary and in the pituitary, and may contribute to elevated levels of FSH in *Taf4b*-null mice, but its normal expression level at 2 wk of age suggests that TAF4B may regulate follistatin in a temporal fashion.

Genome-Wide Expression Profiles of Immature TAF4B-Null Ovaries

A candidate gene approach revealed surprisingly few gene expression changes at 3 wk; thus, we likely missed some novel aspect of transcriptional deregulation within the prepubertal

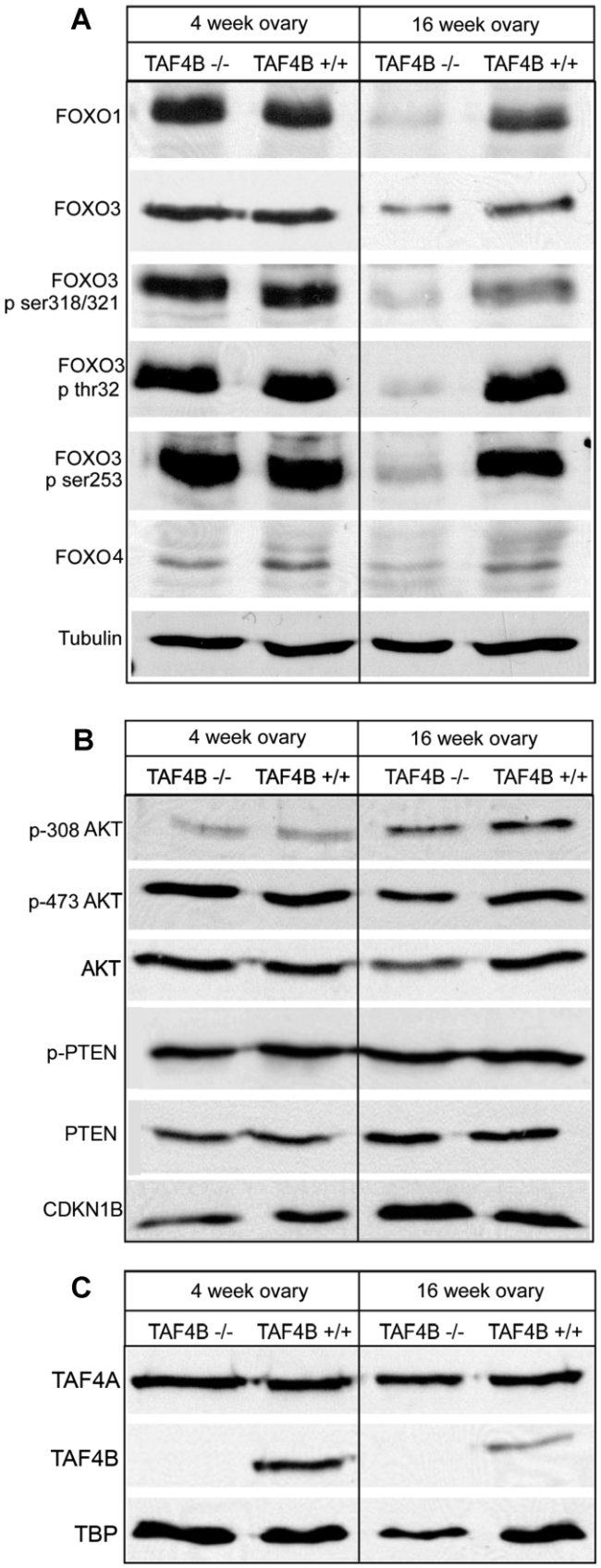

FIG. 3. Age-dependent reduction of key ovarian regulatory proteins in TAF4B-null ovaries. Western blot analysis was used to examine protein levels in the FOXO (**A**), PTEN/AKT pathway (**B**), and TFIID (**C**) using whole-ovary extracts collected from 4- and 16-week-old $TAF4B^{-/-}$ and $TAF4B^{+/+}$ ovaries. An equivalent amount of whole-ovary protein extract was loaded per lane, confirmed by tubulin level (**A**).

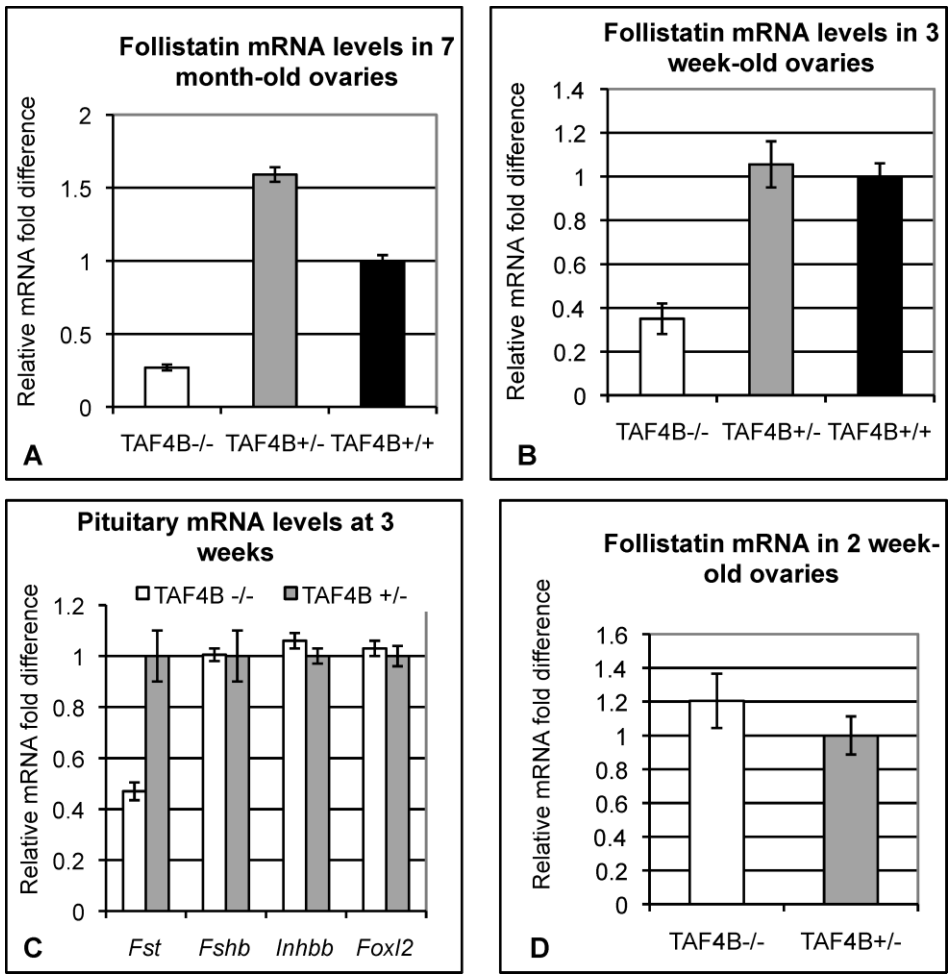

FIG. 4. Defects in TAF4B-null follistatin expression. RNA samples were obtained from 7-mo-old ovaries (**A**), 3-wk-old ovaries (**B**), 3-wk-old pituitaries (**C**), and 2-wk-old ovaries (**D**). Quantitative RT-PCR was used to compare gene expression between *Taf4b*-null cDNA to that derived from heterozygous and/or wild-type littermates. Data were normalized to 18S rRNA present in the cDNA sample. Relative mRNA fold-difference is displayed after setting the wild-type or heterozygote value to one. Error bar represents the SD (**A**–**C**) or SEM (**D**; n = 2 TAF4B$^{+/-}$ and 5 TAF4B$^{-/-}$). *Fshb,* follicle-stimulating hormone subunit beta; *Fst,* follistatin; *Foxl2,* forkhead box protein L2; *Inhbb,* inhibin beta B.

TAF4B-null ovary. To this end, we performed genome-wide expression profiling using microarrays with total RNA derived from the ovaries of 3-wk-old wild-type, heterozygous, and *Taf4b*-null mice in triplicate. By examining this time point, when the ovaries appeared to be healthy, we hoped to obtain an unbiased group of gene expression differences that result more directly from the absence of TAF4B and less from the complete loss of follicles. Of the 28 853 genes represented on the Affymetrix Mouse GeneST GeneChip, 1488 nonredundant genes were present with significant ($P < 0.05$) changes ranging from to 2.7- to 0.27-fold. Complete microarray results can be found at the NCBI GEO under accession number GSE15228. The majority of the gene changes were small. Only 25 genes were expressed in the TAF4B-null ovary at levels 1.5-fold greater than in the wild-type ovary, and 60 genes were down-regulated by 1.5-fold or more. Genes with less than a 1.5-fold difference from wild type were not further analyzed.

Previous expression studies of aging in the ovary have found that the majority of gene changes are reductions [6]. Among the classes down-regulated are mitochondrial and those involved in oxidative stress, DNA metabolism, as well as oocyte-specific genes. Up-regulated genes tended to be involved in receptor binding and immune response/complement activation. The expression changes in TAF4B-null ovaries overlap with the genes disrupted in ovarian aging. Functional annotation analysis of TAF4B-null versus wild-type 3-wk-old ovaries revealed that the main group of down-regulated genes in the TAF4B-null ovary belongs to the Homeobox family and related oocyte transcription factors called the *Obox* family (Table 1). A second down-regulated group includes gene products with nucleotide-binding activity. Within this group are Moloney leukemia virus 10-like 1 (*Mov10l1*) and multiple *Nlrp* genes. The functions of the *Mov10l1* and *Nlrp* genes have not been determined in the ovary. However, they were identified in screens for down-regulated factors in ovary aging [5], and preliminary data hint at important roles in oocyte development and aging [22].

To confirm expression changes identified by the microarray, we used quantitative RT-PCR. Complementary DNA was made from the 3-wk-old ovarian RNA used in the microarray representing biological triplicates for each genotype. Complementary DNA for each genotype was pooled (n = 3 samples/genotype), and quantitative RT-PCR was performed on several interesting genes with roles in folliculogenesis or premature aging (Table 2). We found the largest reduction was of *Mov10l1* (Fig. 5A), with nearly a sixfold reduction from wild type and fourfold reduction from heterozygotes, followed by follistatin (Fig. 4B) and the *Nlrp* genes (Fig. 5A). The reduced level of *Mov10l1* also was present in the ovaries of 2-wk-old TAF4B-null ovaries (Fig. 5B). The majority of fold-changes in the present study were subtle. By examining functional gene groups, we begin to build a picture of how numerous, small gene changes compound to exhibit the defects in TAF4B-null and the aging ovary. Taken together, these data indicate that TAF4B-deficient oocytes display a molecular signature of premature aging and are consistent with the complete infertility of the *Taf4b*-deficient female mice.

TABLE 1. Functional characterization of decreased transcripts in TAF4B-null ovaries at 3 wk.

GenBank accession no.	Gene	Affymetrix fold reduction from WT
Group 1: Homeobox-related		
NM_001038676	*Gm4745,* Similar to oocyte specific homeobox 3	1.96
NR_003269	*Obox 2*	1.77
NM_175342	Cytoplasmic polyadenylated homeobox (*Cphx*)	1.68
NM_008759	*Sebox*	1.56
NM_145709	*Obox5*	1.54
NM_145707	*Obox3*	1.53
NM_011487	Signal transducer and activator of transcription 4	1.52
NM_008262	One cut domain, family member 1, HNF-6	1.50
Group 2: Nucleotide binding proteins		
NM_001004194	NACHT, leucine rich repeat and PYD containing (*Nlrp4e*)	2.70
NM_031260	Moloney leukemia virus 10-like 1	2.22
NM_001042612	*Nlrp9c*	1.99
NM_145216	*Rasl10a*	1.81
NM_001048219	*Nlrp9a*	1.77
NM_145228	2′-5′ Oligoadenylate synthetase 1h	1.67
NM_009449	Tubulin, alpha 3	1.63
NM_007723	Cyclic nucleotide gated channel alpha 1	1.59
NM_029916	Ser thr kinase 31	1.55
NM_172481	*Nlrp4b*	1.52

Ovarian Mov10l1 *expression*

Mov10l1 is a very interesting gene that may play a significant role in the TAF4B-null phenotype. Little is known about this putative RNA helicase, but *Mov10l1* is the mammalian homolog of the *Drosophila* protein, armitage, which has been identified as a germline factor required for RNA interference in the ovary [23, 24]. In mammals, there is tissue-specific expression of *Mov10l1* and its splice variants in the heart, *Champ* and *Csm*. In the mouse testis, *Mov10l1* is expressed at its full length of 25 exons [25, 26]. The heart-specific splice variants, *Champ* and *Csm*, lack the N-terminal coding sequence, and the majority of these proteins are composed only of the helicase domain [26, 27].

To follow up on the reduction of *Mov10l1* in TAF4B-null ovaries, we set out to determine what splice variant is present in the mouse ovary (Fig. 6A). Using quantitative RT-PCR with primers amplifying the N and C terminus regions of *Mov10l1*, we analyzed wild-type mouse testis, heart, and ovary (Fig. 6B). The testis exhibited very high levels of expression of both the N and C termini, whereas heart expression was limited to the C-terminal domain, as shown previously [26]. The 3-wk-old ovary showed expression of both N and C termini, similar to the testis, but at much lower levels. Although well within the detection limits of the assay, juvenile ovary only expressed approximately 1% of the testis *Mov10l1* level. Given that *Mov10l1* is proposed to be restricted to germ cells, lower expression in the ovary is not surprising. Unlike the testis, ovaries contain relatively few germ cells and do not have the ability to repopulate, thereby reducing their oocyte number with age. Indeed, we saw an approximately 10-fold reduction in *Mov10l1* from the 3-wk- to 1-yr-old ovary, consistent with germ cell reduction as ovaries age (Fig. 6B).

To determine if *Mov10l1* expression is directly dependent on TAF4B, we used an siRNA-mediated knockdown approach in vitro. Because *Mov10l1* is expressed in male germ cells, we used the testis germ cell-derived GC1 cell line to evaluate *Mov10l1* expression levels upon TAF4B reduction. GC1 cells were transfected with siRNA targeting either *Taf4a, Taf4b,* or a nontargeting control, followed by 60 h of incubation, at which point target protein levels were reduced by approximately 75% (data not shown) and mRNA levels, while still reduced by approximately 60% (Fig. 6, C and D), were starting to return to normal (24–48 h post-siRNA transfection show the highest *Taf* mRNA reduction). It has been our experience that knockdown of *Taf4b* in cell culture causes an increase in *Taf4a* transcript, which may be a compensatory mechanism (Fig. 6D). *Mov10l1* transcript is elevated 1.3-fold upon knockdown of *Taf4a* and significantly reduced by twofold upon *Taf4b* knockdown, which suggests that its expression is modulated by TAF4B levels (Fig. 6E). *Mov10l1* reduction upon *Taf4b* knockdown is not the effect of global transcriptional down-regulation, because *Tbp* levels remained constant between siRNA targets (Fig. 6F). Perhaps a *Mov10l1* reduction in TAF4B-null oocytes reduces oocyte quality, leading to the appearance of advanced age.

Data about the expression pattern of *Taf4b* within the ovary remain somewhat ambiguous. To suggest that loss of *Taf4b* leads to a reduction of *Mov10l1* in the oocyte, we first need to determine the expression levels of *Taf4b*, *Mov10l1,* and their paralogs in purified populations of ovarian cell types. Using

TABLE 2. Fold changes of selected ovary transcripts between 3-wk TAF4B-null and wild-type (WT) mice by microarray and qRT-PCR.

	Fold of WT	
Gene	Microarray	qRT-PCR
Mov10l1 (murine leukemia virus 10-like 1)	0.45	0.17
Fst (follistatin)	0.62	0.32
Nlrp4e	0.35	0.32
Nlrp9c	0.50	0.37
Xlr5b (X-linked lymphocyte-regulated 5b)	0.52	0.40
Nlrp4b	0.66	0.56
Mael (maelstrom)	0.62	0.70
Ezh2 (enhancer of zeste homlog 2)	0.83	0.72
Taf9b	0.75	0.79
Inhbb (inhibin B)	0.60	0.94
Amh (anti-Mullerian hormone)	0.92	1.00
Foxl2 (forkhead box protein L2)	1.07	1.03
Taf4a	0.93	1.05
Ccnd2 (cyclin D2)	0.89	1.05
Jun (c-jun)	1.09	1.29
Igfbp3 (insulin-like growth factor binding protein 3)	1.25	1.39
Kitl (kit ligand)	1.23	1.61
Lhcgr (luteinizing hormone/choriogonadotropin receptor)	1.47	1.64

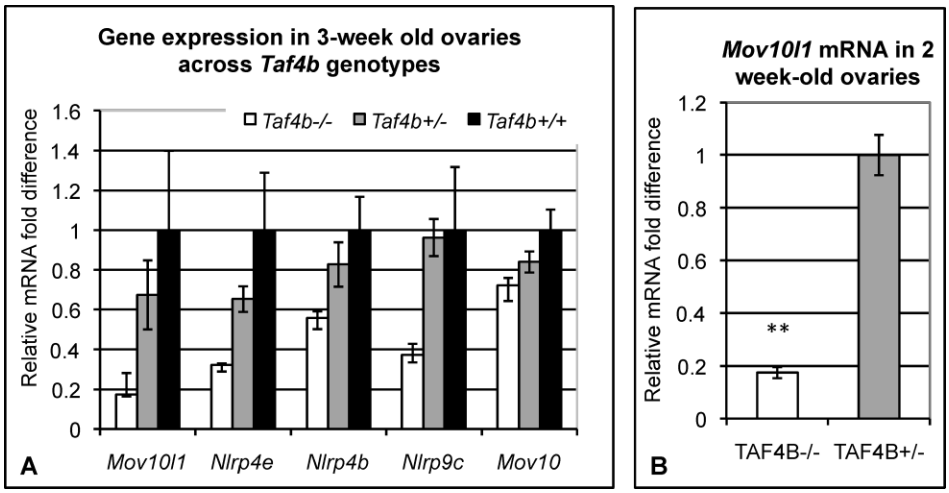

FIG. 5. Confirmation of ovarian gene expression changes from microarray in 3-wk-old TAF4B-null ovaries versus wild-type and heterozygous littermates. **A**) Complementary DNA from the biological triplicate samples used in the microarray were pooled by genotype (*Taf4b*$^{-/-}$, *Taf4b*$^{+/-}$, and *Taf4b*$^{+/+}$) and used in quantitative RT-PCR using gene specific primers. Data was normalized to 18S rRNA present in the cDNA sample. Relative mRNA fold-difference is displayed after setting the TAF4B$^{+/+}$ sample to one. Error bar represents the SD. **B**) *Mov10l1* transcript levels were measured using quantitative RT-PCR from cDNA of 2-wk-old ovaries: TAF4B$^{-/-}$, n = 5; TAF4B$^{+/-}$, n = 2. Data were normalized to 18S rRNA present in the cDNA sample. Relative mRNA fold-difference is displayed after setting the TAF4B$^{+/-}$ sample to one. Error bar represents the SEM. $^{**}P < 0.001$.

quantitative RT-PCR, we compared oocytes, granulosa cells and total ovarian RNA from 8-wk-old wild-type mice for expression of *TAF4a*, *Taf4b*, *Mov10*, and *Mov10l1* (Fig. 7). Here, we normalized to *Actb* (beta-actin) as a more appropriate control when comparing oocytes, which stockpile rRNA [28, 29]. Levels of *Gdf9*, an oocyte-specific transcript, were measured to control for accurate separation of cell types and displayed a 30-fold enrichment over total ovary, whereas detection in granulosa cells was less than 0.09-fold (data not shown). Similarly, *Taf4b* was detected in both oocytes and granulosa cells, with a slight enrichment in oocytes. *Taf4a* showed a significant enrichment in oocytes yet was still expressed in granulosa cells. *Mov10l1* had comparatively very little expression in granulosa cells (0.06-fold of total ovary), but its expression in oocytes was enriched eightfold over total ovary. Unlike its paralog, *Mov10l1*, *Mov10* was present in granulosa cells with only a slight bias toward oocytes. Although this assay did not examine other ovarian cell types, such as epithelial, luteal, or thecal, we now have evidence that *Taf4b* is expressed in both the granulosa cell and oocyte compartments of the adult mouse ovary. We also show, to our knowledge for the first time, that *Mov10l1* is enriched in mammalian oocytes.

Poor oocyte quality often leads to meiotic defects in older women, resulting in aneuploidy [30]. Several genes with confirmed roles in meiosis have been found to have down-regulated transcripts in oocytes of older women, likely contributing to the higher occurrence of chromosomal segregation abnormalities observed. We compared spindle checkpoint protein, *Mad2l1* [31], and kinetochore protein, *Bub1* [32], mRNA levels using quantitative RT-PCR in TAF4B-null and heterozygous 2-wk-old ovaries and a 1-yr-old wild-type mouse ovary. Of these genes, only *Mad2l1* transcripts were reduced in TAF4B-null ovaries compared to their heterozygous siblings, whereas both *Mad2l1* and *Bub1* were further reduced in aged, 1-yr-old wild-type ovaries (Fig. 8). *Mad2l1* expression decreased 3.3-fold from the 2-wk-old TAF4B heterozygous ovaries to the 1-yr-old ovary, consistent with the trend reported in the published data [33]. *Mad2l1* was significantly reduced in TAF4B-null littermate ovaries by approximately 30%. *Bub1* showed a similar pattern of expression, with an eightfold reduction from 2 wk to 1 yr of age, but only showed a 10% reduction from heterozygote to TAF4B-null 2-wk-old ovaries. Chromosomal segregation malfunctions can be caused by the premature separation of sister chromatids because of loss of cohesion. Structural Maintenance of Chromosome (SMC) proteins are integral components of the cohesin complex [34]. Whereas SMC1A is involved in mitosis, SMC1B is meiosis-specific and down-regulated with age [35, 36], contributing to aneuploidy. *Smc1a* expression was equivalent between TAF4B-null and heterozygous 2-wk-old ovaries and the 1-yr-old wild-type ovary (Fig. 8). Expression of *Smc1b* in 1-yr-old wild-type ovaries was very low, with approximately 45-fold less expression than in the 2-wk-old TAF4B heterozygote. Nearly a 60% reduction occurred in *Smc1b* from the 2-wk-old *Taf4b*-heterozygous and *Taf4b*-null mice. This is one of the larger disparities we have documented at such a young age, and it may contribute to the TAF4B-null phenotype. Taken together, the alterations in gene expression are consistent with the hypothesis that TAF4B promotes the correct temporal expression of oocyte-specific genes required for the regulation of oocyte quality and ovarian life span.

DISCUSSION

Unlike other organ systems, the ovary seems to exhibit two distinct aging pathways: age-related oxidative damage, which can be accounted for by the buildup of reactive oxygen species over time, and the reduction of oocyte-specific transcripts, resulting in diminished oocyte quality. Women well below the age of menopause often present with characteristics of older women and require assisted reproductive technology to conceive. This subset of patients undergoing in vitro fertilization may be experiencing advanced ovarian senescence resulting from acceleration of normal ovarian aging pathways. TAF4B is a major regulator of multiple ovarian processes, and disruption of this transcription factor could be an underlying cause of human infertility. In fact, a recent report has linked the integrity of TFIID and *Taf4b* expression levels to oocyte quality in women [37].

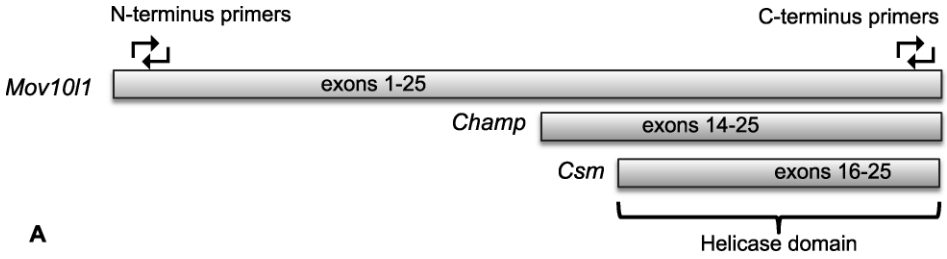

B

	Percentage *Mov10l1* expression vs. testis	
	N-terminus	C-terminus
Adult testis	100± 14.5	100± 16.8
Adult heart	0.0012 ± 0.00008	34.8 ± 0.44
3 week-old ovary	1.37 ± 0.046	0.96 ± 0.11
1 year-old ovary	0.11 ± 0.008	Not tested

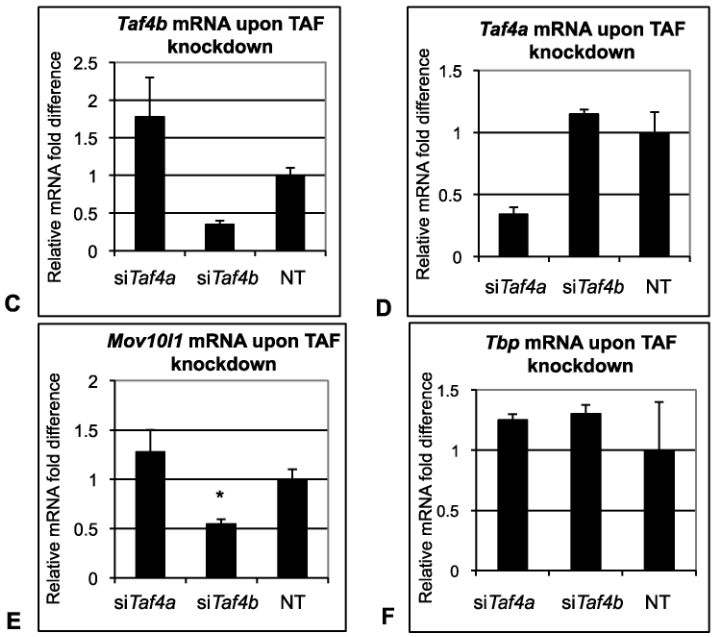

FIG. 6. *Mov10l1* gonad-specific gene expression and TAF4B dependence. **A**) Full-length *Mov10l1* and its splice variants, *Champ* and *Csm*. Of the 25 exons comprising full-length *Mov10l1*, *Champ* is missing the first 13, whereas *Csm* is missing the first 15 and contains only the helicase domain. **B**) Primers specific to the N or C terminus of *Mov10l1*, as diagrammed in **A**, were used in quantitative RT-PCR to determine splice variation between adult testis, adult heart, juvenile ovary (age, 3 wk), and aged ovary (age, 1 yr). With the highest expression of both the N and C termini, adult testis was set to 100% expression. Percentage expression versus testis is indicated with 95% confidence intervals from methodological triplicates. **C**–**F**) *Taf4b* (**C**), *Taf4a* (**D**), *Mov10l1* (**E**), and *Tbp* (**F**) mRNA expression following siRNA knockdown of *Taf4a* and *Taf4b* and using a nontargeting control (NT). Data were normalized to 18S rRNA present in the cDNA sample. Relative mRNA fold-difference is displayed after setting nontargeting value to one. Graphs represent data from two independent trials. Error bar represents the SEM. $*P = 0.03$.

The reproductive defects observed in *Taf4b*-null female mice do not mimic the phenotype of any other transgenic mouse model of infertility. No single developmental block exists; instead, TAF4B seems to be playing a critical role in regulating the timing of multiple reproductive processes. The four major disruptions appear to be with 1) the number of primordial follicles in neonates, 2) the endocrine environment of the ovary beginning in prepubescence, 3) the quality of the mature oocyte, and 4) granulosa cell proliferation and survival. Arguably, the most interesting aspect of the phenotype is that whereas TAF4B is essential for normal transcription in the gonad, it does not appear to be absolutely required for the expression of any one gene at all time points.

In an attempt to find underlying factors that may be disrupted in response to elevated FSH levels, we examined the PTEN/AKT/FOXO pathway. Disruption of the components of this pathway in the TAF4B-null ovary could explain the increases in apoptosis and reduced proliferation in response to FSH [16]. If this pathway were misregulated at an early time point in development, it may explain the loss of follicles in the mature TAF4B-null ovaries. At 4 wk, however, PTEN, AKT, and FOXO proteins are present and phosphorylated in TAF4B-null ovaries at levels very similar to those in wild-type mice, indicating that this pathway is largely intact. As expected, FOXO1 is nearly undetectable in the 16-wk-old TAF4B-null ovary given that FOXO1 expression is concentrated in the granulosa cells of growing follicles [38] and, by this time point, the TAF4B-null ovary is nearly devoid of such follicles. There appears to be a reduction in FOXO3 phosphorylation at 16 wk, which supports our observation of increased apoptosis, but the disruptions in this pathway do not precede but, rather, follow ovary deterioration in the TAF4B knockout.

To uncover gene regulation defects underlying the rapid deterioration of the TAF4B-null ovary, we first took a candidate gene approach, evaluating mRNA levels of genes previously found to be affected by TAF4B expression. Our initial microarray [15] compared TAF4B-null and wild-type ovaries from adult mice. Attempts to recapitulate gene expression changes by quantitative RT-PCR in younger mice were largely unsuccessful, because most genes are expressed at similar levels at 3 wk of age. Both chromatin immunoprecipitation (ChIP) and RT-PCR data using cultured granulosa cell lines have identified TAF4B occupancy at target genes such as *Ccnd2*, *Jun*, *Igfbp3,* and *Fst* [39, 40]. In many cases, genes that

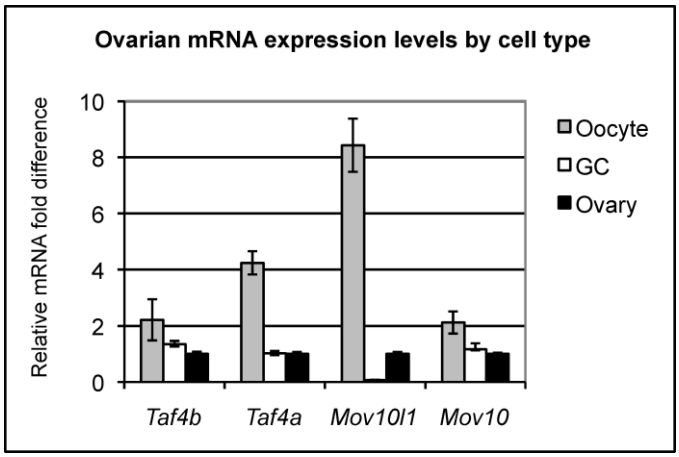

FIG. 7. Ovarian mRNA expression levels by cell type. Oocyte, granulosa cell (GC), or total ovary RNA was collected from 8-wk-old wild-type mice. Quantitative RT-PCR was performed using gene-specific primers for *Taf4b, Taf4a, Mov10l1,* and *Mov10*. Data were normalized to *Actb* mRNA present in the cDNA sample. Relative mRNA fold-difference is displayed after setting the ovary sample to one. Error bars represent the SEM (oocyte, n = 2; GC, n = 3; ovary, n = 3).

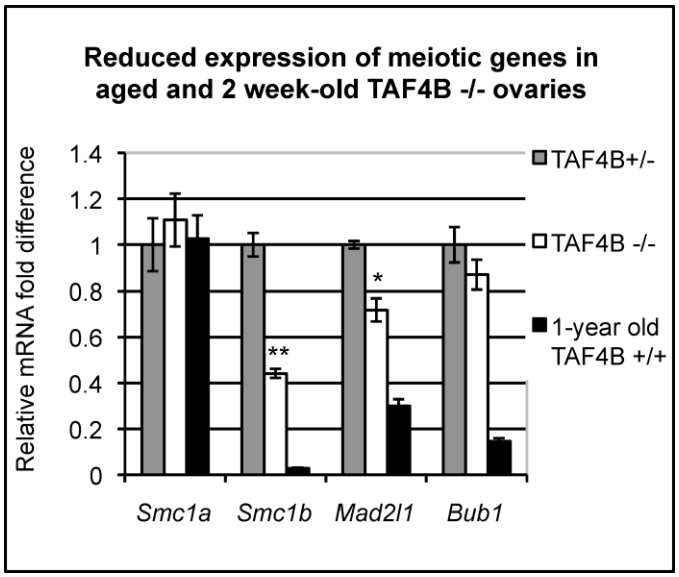

FIG. 8. Reduced expression of meiotic genes in aged and TAF4B-null ovaries. Ovaries from 2-wk-old $Taf4b^{+/-}$ (n = 2) and $Taf4b^{-/-}$ (n = 5) littermates and a 1-yr-old wild-type mouse were used in quantitative RT-PCR using gene-specific primers for *Smc1a, Smc1b, Mad2l1,* and *Bub1*. Data were normalized to 18S rRNA present in the cDNA sample. Relative mRNA fold-difference is displayed after setting the 2-wk-old TAF4B sample to one. Error bar represents the SEM. $*P = 0.02$, $**P < 0.001$.

have shown differential regulation by TAF4B in cultured cells are expressed normally in the *Taf4b*-null mouse at younger ages. However, one gene that was found to be affected both in the present and in previous studies is follistatin, which is reduced by threefold in the 3-wk-old TAF4B-deficient ovary [15, 39]. In fact, *Fst* is up-regulated upon overexpression of TAF4B, and TAF4B, as determined by ChIP, is bound to the *Fst* promoter in cultured granulosa cells [39]. Follistatin is an important negative regulator of activin, thereby acting to suppress FSH release from the pituitary [41]. FSH is consistently elevated in *Taf4b*-null mice [14, 16]. The youngest reported measurement of FSH level in the *Taf4b*-null mouse is 23 days, at which point FSH is elevated [14]. We show here that at 3 wk of age and into adulthood, follistatin is reduced in the *Taf4b*-null mouse. To see if follistatin levels were reduced at even younger ages, we examined 2-wk-old ovaries and pituitaries and found their levels to be equivalent between those of *Taf4b*-null and heterozygous mice. We do not currently know the FSH level of *Taf4b*-null 2-wk-old mice, but it is possible that between 2 and 3 wk of age, follistatin expression is disrupted, leading to the phenotype of elevated FSH. This disruption could stem from a failure of *Taf4b*-null mice to up-regulate follistatin as the first cohort of follicles approaches the antral stage. Alternatively, follistatin may be down-regulated upon entry into estrus, when the ovary starts to receive FSH signals. Because *Taf4b*-null mice enter estrus earlier than their wild-type littermates, this decrease may occur prematurely at 3 wk of age. Thus, regulation of gene expression by TAF4B may be more temporal in nature than expected for a general transcription factor.

Young *Taf4b*-null mice display characteristics of premature ovarian aging, such as persistent estrus, elevated FSH levels, depleted primordial follicle pool, hemorrhagic cysts, fragmented oocytes, poor oocyte quality, and gene expression profiles consistent with advanced oocyte age. Cysts are not prevalent in the C57BL/6 strain, into which the *Taf4b*-null mice have been backcrossed [42]. In the wild-type MRL mouse strain, however, cysts are common, and the incidence of cyst formation increases with age [42]. The etiology of cyst formation is still speculative at this point, but disruptions of genes involved in diverse gonadal function increase their occurrence. Similar cysts have been reported in ovaries of granulosa cell-specific knockouts of follistatin [43], mice lacking the tissue-bound isoform of follistatin [44], granulosa cell-specific knockouts of *Nr5a1* (also known as SF-1) [45], the *Cyp19a1* (also known as aromatase) knockout [46], and mice with chronically high luteinizing hormone levels [47].

To uncover underlying changes in gene expression that may lead to the rapid deterioration of the TAF4B-null ovary, we performed microarray analysis using 3-wk-old ovaries from *Taf4b*-null females and their wild-type and heterozygous siblings. This genome-wide comparison revealed a number of oocyte-specific gene changes that may be indicative of advanced ovarian aging of the TAF4B-null ovary. The most dramatic transcript down-regulated in the knockout, sixfold below that of wild type, was MOV10L1, which is a putative RNA helicase with two splice variants, *Csm* and *Champ*, that are involved in heart development [26]. The full-length *Mov10l1*, isoform 1, was once identified as a testis germ cell-specific gene [25], but expressed sequence tags (ESTs) have since been identified in oocytes in mice, frogs, and humans. MOV10L1 shares a very high degree of homology with the *Drosophila* protein, armitage [48]. Disruptions in armitage lead to male and female sterility because of a RNA-induced silencing complex (RISC) maturation failure [24]. Here, we show that not only the mouse testis but also the ovary expresses *Mov10l1*; that its expression is decreased in aged ovaries, presumably because of lower oocyte number; and that its expression is dependent on TAF4B.

An interesting and unexpected finding was the reduction of a number of *Nlrp* (NACHT, leucine-rich repeat and PYD-containing), also referred to as NALP, genes. The *Nlrp* family, identified in a screen for genes involved in oocyte aging [5], is composed of 14 members in humans and 20 members in mice, presumably stemming from several gene duplication events [49]. The *Nlrp* genes belong to a superfamily of NOD-like receptors, which have roles in inflammation and innate immunity. Many of these genes are specifically expressed in

the ovary, and loss of function in *Nlrp5* (Mater), *Nlrp4*, *Nlrp7*, or *Nlrp14* has been shown to cause female reproductive failure [49]. In the TAF4B-null ovary, *Nlrp4e, Nlrp9c,* and *Nlrp4b* were confirmed by RT-PCR to be reduced by 3.11-, 2.68-, and 1.79-fold, respectively. Interestingly, many of the *Nlrp* genes are clustered on chromosome 7 [49], very close to the location of the *Obox* genes, which also are down-regulated in the TAF4B-null ovary. Factor in the germline alpha (FIGLA), a critical oocyte transcription factor, also regulates the expression of several *Nlrp* genes [50]. Roles for *Nlrp* genes in oocyte and preimplantation development and innate immunity have been established, but functional data are scarce. Given that expression of these genes is decreased with oocyte age and is regulated by two critical ovarian transcription factors, TAF4B and FIGLA, the *Nlrp* family may prove to be very interesting with respect to reproduction and aging.

It is evident that the reduced number of primordial follicles in the TAF4B-null oocytes contributes to the very early depletion observed by 17 wk. TAF4B-null ovaries from pnd 1 mice contain the same number of primordial follicles as their fertile littermates, but by pnd 3, this number is reduced [14]. Interestingly, no increase in apoptosis is observed, leading us to question what has happened to these oocytes. A recent study on germ cell loss in the perinatal mouse has highlighted the role of autophagy in the initial wave of germ cell culling that takes place after birth [51]. Indeed, the microarray in the present study showed a slight increase in autophagy-related genes, which may be responsible for the lower number of germ cells in TAF4B-null ovaries, but this supposition requires much further work. Thus, a complex syndrome of ovarian defects that occurs from shortly after birth and into adulthood culminates in premature reproductive senescence and infertility in the absence of TAF4B.

The emergence of *Smc1b* as a disrupted gene in TAF4B-null ovaries offers new mechanistic possibilities to explain infertility. Reduction of *Smc1b* results in cohesion complexes that are unable to maintain attachments between sister chromatids, leading to premature segregation that results in oocyte death. Targeted deletion of *Smc1b* yields infertile mice, and deletion of *Spo11*, an important factor required for meiotic chromosome synapsis, results in a very similar phenotype to that of *Taf4b*-null females [34, 52].

The precise mechanism of how loss of *Taf4b* in mice leads to advanced ovarian age remains to be determined. The microarray performed in the present study on prepubescent mice provides a new set of possible TAF4B-target genes involved in regulation of ovarian life span. Oocyte aging is not only regulated by factors within the germ cell but also profoundly influenced by the follicular microenvironment [53, 54]. Elucidating how TAF4B acts in granulosa cells, oocytes, or both to maintain proper timing of ovarian events will yield insight regarding normal regulation of ovarian aging and may uncover new therapeutic opportunities for women who experience premature reproductive senescence and infertility.

ACKNOWLEDGMENTS

We thank Mary Hixon, Aron Gyuris, and Diana Donovan for helpful suggestions during the course of these studies and comments on the manuscript. We thank Paula Weston and Michele Gardner of the Molecular Pathology Core facility at Brown for ovarian histology.

REFERENCES

1. Faddy MJ, Gosden RG, Gougeon A, Richardson SJ, Nelson JF. Accelerated disappearance of ovarian follicles in midlife: implications for forecasting menopause. Hum Reprod 1992; 7:1342–1346.
2. Levi AJ, Raynault MF, Bergh PA, Drews MR, Miller BT, Scott RT Jr. Reproductive outcome in patients with diminished ovarian reserve. Fertil Steril 2001; 76:666–669.
3. Sauer MV. The impact of age on reproductive potential: lessons learned from oocyte donation. Maturitas 1998; 30:221–225.
4. Pan H, Ma P, Zhu W, Schultz RM. Age-associated increase in aneuploidy and changes in gene expression in mouse eggs. Dev Biol 2008; 316:397–407.
5. Hamatani T, Falco G, Carter MG, Akutsu H, Stagg CA, Sharov AA, Dudekula DB, VanBuren V, Ko MS. Age-associated alteration of gene expression patterns in mouse oocytes. Hum Mol Genet 2004; 13:2263–2278.
6. Sharov AA, Falco G, Piao Y, Poosala S, Becker KG, Zonderman AB, Longo DL, Schlessinger D, Ko M. Effects of aging and calorie restriction on the global gene expression profiles of mouse testis and ovary. BMC Biol 2008; 6:24.
7. Xiao L, Kim M, DeJong J. Developmental and cell type-specific regulation of core promoter transcription factors in germ cells of frogs and mice. Gene Expr Patterns 2006; 6:409–419.
8. Hiller M, Chen X, Pringle MJ, Suchorolski M, Sancak Y, Viswanathan S, Bolival B, Lin TY, Marino S, Fuller MT. Testis-specific TAF homologs collaborate to control a tissue-specific transcription program. Development 2004; 131:5297–5308.
9. Freiman RN. Specific variants of general transcription factors regulate germ cell development in diverse organisms. Biochimica Biophys Acta 2009 (1789):161–166.
10. Albright SR, Tjian R. TAFs revisited: more data reveal new twists and confirm old ideas. Gene 2000; 242:1–13.
11. Roeder RG. The role of general initiation factors in transcription by RNA polymerase II. Trends Biochem Sci 1996; 21:327–335.
12. Verrijzer CP, Tjian R. TAFs mediate transcriptional activation and promoter selectivity. Trends Biochem Sci 1996; 21:338–342.
13. Falender AE, Freiman RN, Geles KG, Lo KC, Hwang K, Lamb DJ, Morris PL, Tjian R, Richards JS. Maintenance of spermatogenesis requires TAF4b, a gonad-specific subunit of TFIID. Genes Dev 2005; 19:794–803.
14. Falender AE, Shimada M, Lo YK, Richards JS. TAF4b, a TBP-associated factor, is required for oocyte development and function. Dev Biol 2005; 288:405–419.
15. Freiman RN, Albright SR, Zheng S, Sha WC, Hammer RE, Tjian R. Requirement of tissue-selective TBP-associated factor TAFII105 in ovarian development. Science 2001; 293:2084–2087.
16. Voronina E, Lovasco LA, Gyuris A, Baumgartner RA, Parlow AF, Freiman RN. Ovarian granulosa cell survival and proliferation requires the gonad-selective TFIID subunit TAF4b. Dev Biol 2007; 303:715–726.
17. Rajkovic A, Yan C, Yan W, Klysik M, Matzuk MM. Obox, a family of homeobox genes preferentially expressed in germ cells. Genomics 2002; 79:711–717.
18. Ebert KM, Paynton BV, McKnight GS, Brinster RL. Translation and stability of ovalbumin messenger RNA injected into growing oocytes and fertilized ova of mice. J Embryol Exp Morphol 1984; 84:91–103.
19. Dennis G Jr, Sherman BT, Hosack DA, Yang J, Gao W, Lane HC, Lempicki RA. DAVID: Database for Annotation, Visualization, and Integrated Discovery. Genome Biol 2003; 4:P3.
20. Selesniemi K, Lee HJ, Tilly JL. Moderate caloric restriction initiated in rodents during adulthood sustains function of the female reproductive axis into advanced chronological age. Aging Cell 2008; 7:622–629.
21. Gospodarowicz D, Lau K. Pituitary follicular cells secrete both vascular endothelial growth factor and follistatin. Biochem Biophys Res Commun 1989; 165:292–298.
22. Evsikov AV, Graber JH, Brockman JM, Hampl A, Holbrook AE, Singh P, Eppig JJ, Solter D, Knowles BB. Cracking the egg: molecular dynamics and evolutionary aspects of the transition from the fully grown oocyte to embryo. Genes Dev 2006; 20:2713–2727.
23. Cook HA, Koppetsch BS, Wu J, Theurkauf WE. The *Drosophila* SDE3 homolog armitage is required for oskar mRNA silencing and embryonic axis specification. Cell 2004; 116:817–829.
24. Tomari Y, Du T, Haley B, Schwarz DS, Bennett R, Cook HA, Koppetsch BS, Theurkauf WE, Zamore PD. RISC assembly defects in the *Drosophila* RNAi mutant armitage. Cell 2004; 116:831–841.
25. Wang PJ, McCarrey JR, Yang F, Page DC. An abundance of X-linked genes expressed in spermatogonia. Nat Genet 2001; 27:422–426.
26. Ueyama T, Kasahara H, Ishiwata T, Yamasaki N, Izumo S. Csm, a cardiac-specific isoform of the RNA helicase Mov10l1, is regulated by Nkx2.5 in embryonic heart. J Biol Chem 2003; 278:28750–28757.
27. Liu ZP, Nakagawa O, Nakagawa M, Yanagisawa H, Passier R, Richardson JA, Srivastava D, Olson EN. CHAMP, a novel cardiac-specific helicase regulated by MEF2C. Dev Biol 2001; 234:497–509.
28. Tian Q, Kopf GS, Brown RS, Tseng H. Function of basonuclin in

increasing transcription of the ribosomal RNA genes during mouse oogenesis. Development 2001; 128:407–416.
29. Kaplan G, Abreu SL, Bachvarova R. rRNA accumulation and protein synthetic patterns in growing mouse oocytes. J Exp Zool 1982; 220:361–370.
30. Hassold T, Hunt P. To err (meiotically) is human: the genesis of human aneuploidy. Nat Rev Genet 2001; 2:280–291.
31. Niault T, Hached K, Sotillo R, Sorger PK, Maro B, Benezra R, Wassmann K. Changing Mad2 levels affects chromosome segregation and spindle assembly checkpoint control in female mouse meiosis I. PLoS ONE 2007; 2(11):e1165.
32. Yin S, Wang Q, Liu JH, Ai JS, Liang CG, Hou Y, Chen DY, Schatten H, Sun QY. Bub1 prevents chromosome misalignment and precocious anaphase during mouse oocyte meiosis. Cell Cycle 2006; 5:2130–2137.
33. Steuerwald NM, Steuerwald MD, Mailhes JB. Postovulatory aging of mouse oocytes leads to decreased MAD2 transcripts and increased frequencies of premature centromere separation and anaphase. Mol Hum Reprod 2005; 11:623–630.
34. Revenkova E, Eijpe M, Heyting C, Hodges CA, Hunt PA, Liebe B, Scherthan H, Jessberger R. Cohesin SMC1 beta is required for meiotic chromosome dynamics, sister chromatid cohesion and DNA recombination. Nat Cell Biol 2004; 6:555–562.
35. Liu L, Keefe DL. Defective cohesin is associated with age-dependent misaligned chromosomes in oocytes. Reprod Biomed Online 2008; 16: 103–112.
36. Cukurcam S, Betzendahl I, Michel G, Vogt E, Hegele-Hartung C, Lindenthal B, Eichenlaub-Ritter U. Influence of follicular fluid meiosis-activating sterol on aneuploidy rate and precocious chromatid segregation in aged mouse oocytes. Hum Reprod 2007; 22:815–828.
37. Di Pietro C, Vento M, Ragusa M, Barbagallo D, Guglielmino MR, Maniscalchi T, Duro LR, Tomasello L, Majorana A, De Palma A, Borzì P, Scollo P, Purrello M. Expression analysis of TFIID in single human oocytes: new potential molecular markers of oocyte quality. Reprod Biomed Online 2008; 17:338–349.
38. Shi F, LaPolt PS. Relationship between FoxO1 protein levels and follicular development, atresia, and luteinization in the rat ovary. J Endocrinol 2003; 179:195–203.
39. Geles KG, Freiman RN, Liu WL, Zheng S, Voronina E, Tjian R. Cell-type-selective induction of c-jun by TAF4b directs ovarian-specific transcription networks. Proc Natl Acad Sci U S A 2006; 103:2594–2599.
40. Ongeri EM, Verderame MF, Hammond JM. The TATA binding protein associated factor 4b (TAF4b) mediates FSH stimulation of the IGFBP-3 promoter in cultured porcine ovarian granulosa cells. Mol Cell Endocrinol 2007; 278:29–35.
41. Nakamura T, Takio K, Eto Y, Shibai H, Titani K, Sugino H. Activin-binding protein from rat ovary is follistatin. Science 1990; 247:836–838.
42. Kon Y, Konno A, Hashimoto Y, Endoh D. Ovarian cysts in MRL/MpJ mice originate from rete ovarii. Anat Histol Embryol 2007; 36:172–178.
43. Jorgez CJ, Klysik M, Jamin SP, Behringer RR, Matzuk MM. Granulosa cell-specific inactivation of follistatin causes female fertility defects. Mol Endocrinol 2004; 18:953–967.
44. Lin SY, Craythorn RG, O'Connor AE, Matzuk MM, Girling JE, Morrison JR, de Kretser DM. Female infertility and disrupted angiogenesis are actions of specific follistatin isoforms. Mol Endocrinol 2008; 22:415–429.
45. Jeyasuria P, Ikeda Y, Jamin SP, Zhao L, De Rooij DG, Themmen AP, Behringer RR, Parker KL. Cell-specific knockout of steroidogenic factor 1 reveals its essential roles in gonadal function. Mol Endocrinol 2004; 18: 1610–1619.
46. Britt KL, Drummond AE, Cox VA, Dyson M, Wreford NG, Jones ME, Simpson ER, Findlay JK. An age-related ovarian phenotype in mice with targeted disruption of the Cyp 19 (aromatase) gene. Endocrinology 2000; 141:2614–2623.
47. Risma KA, Hirshfield AN, Nilson JH. Elevated luteinizing hormone in prepubertal transgenic mice causes hyperandrogenemia, precocious puberty, and substantial ovarian pathology. Endocrinology 1997; 138: 3540–3547.
48. Altschul SF, Madden TL, Schäffer AA, Zhang J, Zhang Z, Miller W, Lipman DJ. Gapped BLAST and PSI-BLAST: a new generation of protein database search programs. Nucleic Acids Res 1997; 25:3389–3402.
49. Martinon F, Gaide O, Petrilli V, Mayor A, Tschopp J. NALP inflammasomes: a central role in innate immunity. Semin Immunopathol 2007; 29:213–229.
50. Soyal SM, Amleh A, Dean J. FIGalpha, a germ cell-specific transcription factor required for ovarian follicle formation. Development 2000; 127: 4645–4654.
51. Rodrigues P, Limback D, McGinnis LK, Plancha CE, Albertini DF. Multiple mechanisms of germ cell loss in the perinatal mouse ovary. Reproduction 2009; 137:709–720.
52. Baudat F, Manova K, Yuen JP, Jasin M, Keeney S. Chromosome synapsis defects and sexually dimorphic meiotic progression in mice lacking Spo11. Mol Cell 2000; 6:989–998.
53. Qiao TW, Liu N, Miao DQ, Zhang X, Han D, Ge L, Tan JH. Cumulus cells accelerate aging of mouse oocytes by secreting a soluble factor(s). Mol Reprod Dev 2008; 75:521–528.
54. Tatone C, Amicarelli F, Carbone MC, Monteleone P, Caserta D, Marci R, Artini PG, Piomboni P, Focarelli R. Cellular and molecular aspects of ovarian follicle ageing. Hum Reprod Update 2008; 14:131–142.